Australian Government
Department of Agriculture, Water and the Environment
Supervising Scientist

internal report **665**

Gamma dose rates and radon-222 exhalation flux densities at El Sherana containment in 2019

Scott McMaster, Jefferson Chen, John Pfitzner, Che Doering

June 2021

Release status – Unrestricted

Project number – MON-2013-006

The Department acknowledges the traditional owners of country throughout Australia and their continuing connection to land, sea and community. We pay our respects to them and their cultures and to their elders both past and present.

Gamma dose rates and radon-222 exhalation flux densities at El Sherana containment in 2019

Scott McMaster, Jefferson Chen, John Pfitzner, Che Doering

Supervising Scientist

GPO Box 461, Darwin NT 0801

June 2021

(Release status – Unrestricted)

Australian Government

Department of Agriculture, Water and the Environment

Supervising Scientist

How to cite this report:

McMaster S, Chen J, Pfitzner J & Doering C 2021. Gamma dose rates and radon-222 exhalation flux densities at El Sherana containment in 2019. Internal Report 665, June 2021, Supervising Scientist, Darwin.

Project number: (MON-2013-006)

Authors of this report:

Scott McMaster – Supervising Scientist, GPO Box 461, Darwin NT 0801, Australia

Jefferson Chen –Supervising Scientist, GPO Box 461, Darwin NT 0801, Australia

John Pfitzner – Supervising Scientist, GPO Box 461, Darwin NT 0801, Australia

Che Doering – Supervising Scientist, GPO Box 461, Darwin NT 0801, Australia

Supervising Scientist is a branch of the Australian Government Department of Agriculture, Water and the Environment.

Supervising Scientist
Department of Agriculture, Water and the Environment
GPO Box 461, Darwin NT 0801 Australia

environment.gov.au/science/supervising-scientist/publications

Executive summary

Gamma dose rates and radon-222 exhalation fluxes are measured at the El Sherana containment every two years to provide ongoing assurance that radioactive waste material buried at the facility does not present an unacceptable radiation health risk to Parks Australia employees or the public. This report presents the measurements from June 2019, the sixth set of measurements since construction of the containment in 2009. Average gamma dose rates and radon-222 exhalation flux densities in 2019 were no different to baseline values in 2007 before the containment was built. Consequently, the levels measured in 2019 would not result in above-background doses to Parks Australia employees or the public above the dose constraint of 30 μSv per year. The implication of these results is that there is currently no unacceptable radiation health risk associated with buried radioactive waste material at the containment.

1 Introduction

The El Sherana containment is a near-surface disposal facility located in the South Alligator River valley in the southern part of Kakadu National Park. It was constructed in the 2009 dry season and contains approximately 22,000 m^3 of radioactively contaminated waste from the remediation of legacy uranium mining and processing sites in the area. Engineering details of the containment are summarised in Doering et al (2011) and Bollhöfer et al (2013, 2015). The uranium mining history of the South Alligator River valley is summarised in Waggitt (2004).

The El Sherana containment is currently in the institutional control period, during which time, public access to the site must be restricted and the site must not be used for other purposes (NHMRC 1993). The site is managed by the Director of National Parks, with regulatory oversight by the Australian Radiation Protection and Nuclear Safety Agency (ARPANSA). The Supervising Scientist assists the Director of National Parks with radiological monitoring of the site by conducting biennial measurements of gamma dose rates and radon-222 exhalation flux densities.

A dose constraint of 30 $\mu Sv\ y^{-1}$ for both public and occupational exposure has been set for the El Sherana containment based on an assessment of plausible exposure scenarios (Bollhöfer et al 2013). The dose constraint represents an upper bound on the expected above-background doses from the containment and a level below which radiation exposures should be optimised (ICRP 2007).

This report presents the results of gamma dose rate and radon exhalation flux density measurements conducted in May/June 2019 and compares them to previous measurement results, including baseline values measured in 2007. Based on these results, we have determined the potential for above-background radiation doses to workers and the public, and also the acceptability of such exposures in the context of the dose constraint.

2 Methods

2.1 Radon-222 exhalation flux densities

Radon-222 exhalation flux densities were measured over the period 30th May to 3rd June 2019. The prevailing meteorological conditions during the measurement period were typical of the tropical Northern Territory dry season, with maximum daytime temperatures around 30°C and zero rainfall.

Brass canisters containing activated charcoal were used for field sampling of radon-222 exhalation flux densities. The canisters were prepared by heating in an oven at 110°C for 48 hours to drive out residual radon-222 adsorbed on the surface of the charcoal. They were then allowed to cool to room temperature and immediately sealed for transport to the field.

Forty six canisters were deployed on and around the containment and their geospatial coordinates recorded using a global positioning system (GPS). The canisters were embedded in the ground surface to a depth of approximately 1 cm to trap exhaling radon-222. Two additional canisters were carried into the field but remained sealed at all times. These canisters were ‘controls’ and used to determine the background activity of radon-222 on the charcoal.

At the end of the sampling period, the canisters were removed from the ground surface and immediately sealed for transport back to the laboratory. They were then counted for a period of 600 s on sodium iodide (NaI) and high purity germanium (HPGe) gamma detectors and the resulting energy spectrum displayed on a multi-channel analyser. The control and calibration standard canisters were also counted. Regions of interest were established around the characteristic photopeaks of the radon-222 decay products lead-214 (242 keV, 295 keV and 352 keV) and bismuth-214 (609 keV).

The net count rate of these decay products in the field samples was determined by summing the total counts under each peak region of interest and then subtracting the arithmetic mean of the total counts under the corresponding regions of interest for the two control canisters. The counting efficiency of the detector was determined to be 10.3% using a sealed canister containing charcoal spiked with a known activity of radium-226, the parent radionuclide of radon-222.

Radon-222 exhalation flux densities were calculated following the method described in Spehr & Johnston (1983) as:

$$J = \frac{R \cdot t_c \cdot \lambda^2 \cdot \exp(\lambda \cdot t_d)}{\varepsilon \cdot a \cdot [1 - \exp(-\lambda \cdot t_s)] \cdot [1 - \exp(-\lambda \cdot t_c)]}$$

where J (Bq m^{-2} s^{-1}) is the average radon-222 flux density, R (s^{-1}) is the net count rate of radon-222 decay products, t_c (s) is the counting period, λ (s^{-1}) is the radon-222 decay constant, t_d (s) is the delay period from the end of sampling to the beginning of counting, ε (s^{-1} Bq^{-1}) is the counting efficiency of the detector, a (m^2) is the area of the open face of the canister when embedded in the ground and t_s (s) is the duration of the sampling period.

2.2 Gamma dose rates

Total gamma counts were measured on 30 May 2019 at each location where charcoal canisters were deployed. The count time was 60 s and the height of the measurement was approximately 1 m above the ground surface. A RadEye GX meter with an attached Mini Instrument MC70 Geiger Müller tube was used to make the measurements. This meter (GM2) was calibrated by an external laboratory (SafeRadiation) against a certified radiation source. Gamma counts recorded during the field survey were then converted to an absorbed dose rate using:

$$D = \frac{C}{T} \times \frac{1}{15.5} \times \frac{1}{1.21}$$

Where:

D (µGy h^{-1}) is the absorbed dose rate;

C (counts) is the number of counts recorded by the meter normalised to GM2;

T (s) is the time over which field counts were recorded;

15.5 (counts s^{-1} per µSv h^{-1}) is the count rate to effective dose rate conversion factor reported on the calibration certificate of GM2; and

1.21 (Sv Gy^{-1}) is the effective to absorbed dose conversion factor reported on the calibration certificate of GM2.

3 Results and discussion

Figure 1 shows the location and magnitude of the radon-222 exhalation flux density measurements and Figure 2 shows the gamma dose rate measurements. The raw data underpinning these figures is provided in Appendix 1.

Radon-222 exhalation flux densities were measured in three zones: on the containment, off the containment but inside the fenced area, and outside the fenced area (Figure 1). The arithmetic mean and standard deviation radon-222 exhalation flux density on the containment was 6.58 ± 9.45 mBq m^{-2} s^{-1} (n = 29), although this value was skewed by one outlier which had an exhalation flux of 49.1 mBq m^{-2} s^{-1}. The geometric mean value of 3.71 mBq m^{-2} s^{-1} is perhaps more representative of the average radon-222 exhalation flux density on the containment, as less weight is placed on outliers.

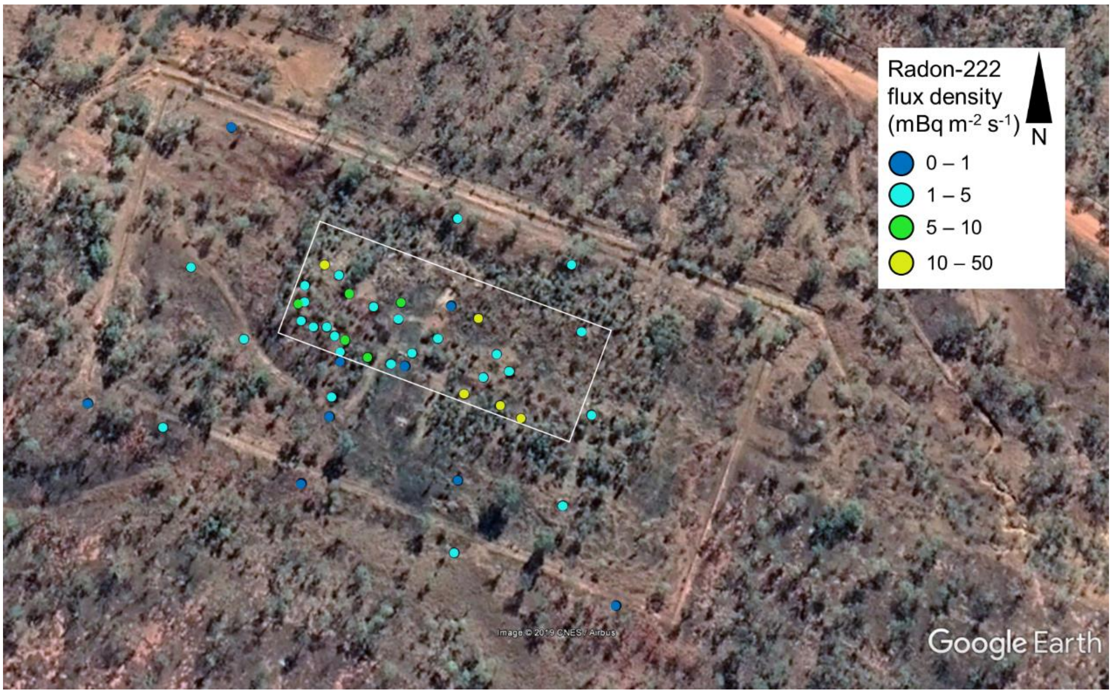

Figure 1 *Radon-222 exhalation flux densities measured at the measured at the South Alligator Containment Facility in May/June 2019 (the white rectangular outline indicates the location of the containment).*

In five locations on the containment, elevated levels (>10 mBq m^{-2} s^{-1}) of radon exhalation flux density were measured. These points did not correspond with elevated gamma dose rates, suggesting that the sampled radon-222 at these locations may have originated from deeper in the soil profile, possibly from the buried waste itself through cracks in the clay cap. Radon-222 in dry soil has a diffusion length of about 1.5 m (IAEA 2013, Porstendörfer 1994), making it possible for radon-222 generated by the decay of radium-226 in the buried waste to be exhaled from the surface of the containment. By comparison, the gamma signal in air at 1 m above the ground generally comes from radionuclides located in about the top 0.5 m of the soil, with deeper lying radionuclides tending to contribute only a few percent or less (ICRU 1994).

Gamma dose rates in the three zones were effectively the same (Figure 2). The arithmetic mean and standard deviation gamma dose rate on the containment was 0.12 ± 0.01 μGy h^{-1} (n = 30), off the containment but inside the fenced area was 0.12 ± 0.01 μGy h^{-1} (n = 11) and outside the fenced area was 0.13 ± 0.03 μGy h^{-1} (n = 5). The slightly higher arithmetic mean dose rate outside the fenced area was due to one outlier which was included in the calculation. In this case, the geometric mean for outside the fenced area of 0.12 μGy h^{-1} may be more representative.

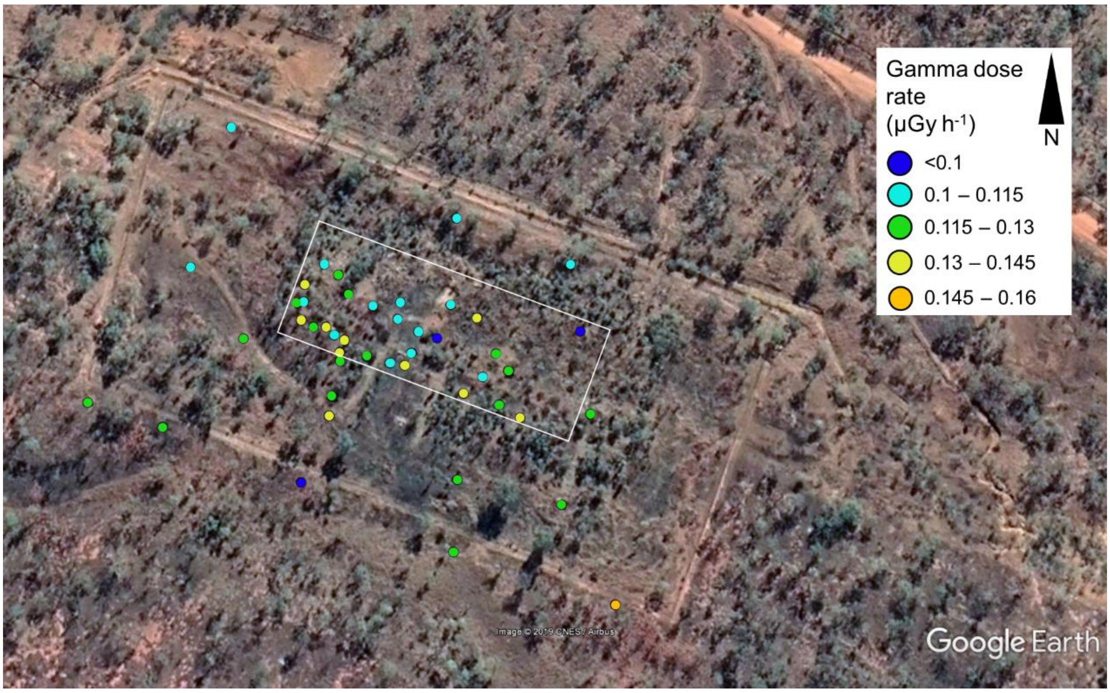

Figure 2 *Gamma dose rates measured South Alligator Containment Facility in May 2019 (the white rectangular outline indicates the location of the containment).*

Table 1 compares the 2019 radon-222 exhalation flux densities on the containment to previous measurements, including baseline values from 2007. Radon-222 exhalation flux densities on the containment have typically been higher than baseline values and variable between years, though showing a decreasing trend since 2012 (Figure 3).

Both the arithmetic and geometric mean of the 2019 measurements was less than the geometric mean baseline value, implying there was no above-background radon-222 exposure pathway to workers or the public at the time of measurements. In work published by the IAEA, vegetated sites were shown to have higher radon flux densities due to decreased soil moisture contents and root intrusion causing increase the permeability of the soil (IAEA 2013). As the baseline measurements conducted in 2007 were carried out on a vegetated site, this could potentially explain the slightly elevated radon exhalation flux densities in the baseline study in comparison to the current work.

Table 1 *Summary of biennial radon exhalation flux densities (mBq m^{-2} s^{-1}) on the containment*

Year	Arithmetic mean	Arithmetic standard deviation	Geometric mean	Geometric standard deviation	Minimum	Maximum	*n*
2007[a]	14	6	13	1.5	5.0	25	21
2010	29	39	19	2.8	6.2	170	34
2012	240	230	120	2.2	18	750	17
2013	180	150	99	2.1	9.7	530	30
2015	110	90	72	3.0	5.0	350	30
2017	29	70	7.1	2.9	0.19	320	31
2019	7	9	4	2.9	0.5	49	29

[a]Baseline measurements

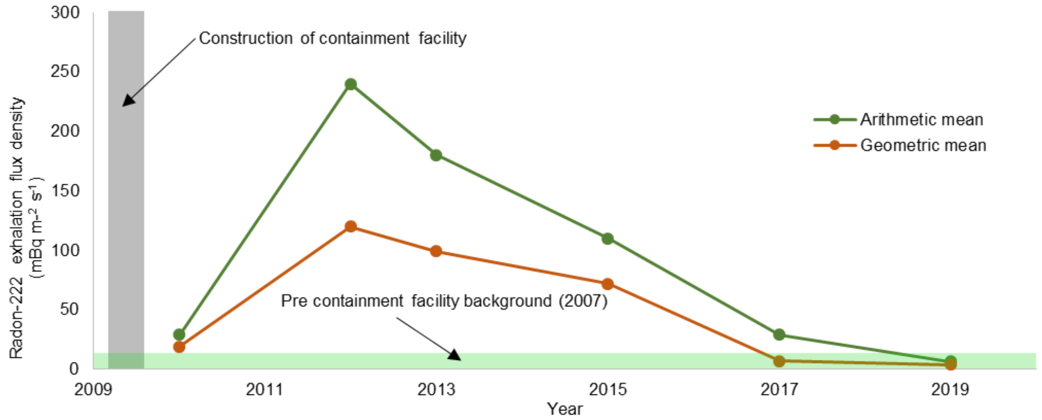

***Figure 3** Mean radon-222 exhalation flux density changes on the containment since construction*

Variability in radon-222 exhalation flux densities between years may be due to a number of factors, including changes in containment surface soil and vegetation cover and differences in the timing of biennial measurements. The original ~2.5 m thick surface soil layer (or 'growth medium') on the containment was supplemented by an additional 1 m of soil in 2013 and the surface re-contoured following erosion in the previous wet seasons. Vegetation cover on the containment has varied from being bare in 2010 and 2013, dense with grass and scrub in 2015 and sparse in 2017 due to a recent fire (Doering et al. 2017). In 2019, there was dense grass and vegetation covering the majority of the containment area, except for in the south west corner where little vegetation was noted.

Radon-222 measurements in 2015, 2017 and 2019 were taken early in the dry season (May and June) and were lower than those in 2010–2013, taken late in the dry season (September and October) (Table 1). Soil moisture content can be higher in the early dry season, immediately following the wet season. Higher soil moisture content is known to result in lower radon-222 exhalation from a substrate (Bollhöfer & Doering 2016), as it impedes the emanation of radon-222 from the soil grain into the soil pore space (IAEA 2013, Porstendörfer 1994).

An additional factor which can influence radon-222 exhalation fluxes is consolidation of the soil on the containment. In this process, soil volume decreases gradually due to changes in soil pore water pressure. As the density of the soil gradually increases this can result in less pore space and hence decrease the diffusion length of radon through the soil. A decreased radon diffusion length results in lower radon-222 exhalation fluxes.

Table 2 compares the 2019 gamma dose rates on the containment to previous measurements, including baseline values from 2007. Gamma dose rates have effectively remained unchanged from baseline values. The implication is that gamma radiation from radionuclides in the buried waste has been effectively attenuated by the clay cap and surface soil layer and that to date there has been no above-background gamma exposure pathway to workers or the public from the containment.

***Table 2** Summary of biennial gamma dose rates (µGy h^{-1}) on the containment*

Year	Arithmetic mean	Arithmetic standard deviation	Geometric mean	Geometric standard deviation	Minimum	Maximum	*n*
2007[a]	0.12	0.01	0.12	1.1	0.09	0.14	100

2010	0.1	0.01	0.1	1.1	0.08	0.13	230
2012	0.13	0.01	0.13	1.1	0.1	0.17	202
2013	0.13	0.01	0.13	1.1	0.11	0.15	30
2015	0.13	0.01	0.13	1.1	0.1	0.14	30
2017	0.13	0.01	0.13	1.1	0.11	0.15	31
2019	0.12	0.01	0.12	1.1	0.09	0.14	30

[a]Baseline measurements

No dose modelling using the 2019 measurements was conducted, as the results indicated there was effectively no above-background radon-222 or gamma exposure pathway to workers or the public. Thus, the outcome of dose modelling using the measurement results would be a zero dose.

4 Conclusion

Average radon-222 exhalation flux densities and gamma dose rates at the El Sherana containment in 2019 were effectively no different to baseline values from 2007. The conclusion is that there was no above-background radon-222 or gamma exposure pathway to workers or the public at the time of measurements and there would be no exceedance of the occupational or public dose constraint of 30 μSv y^{-1} for the containment. Measurements of radon-222 exhalation flux densities and gamma dose rates at the containment should continue into the future to provide ongoing assurance of the performance of the facility and to ensure that workers and the public remain protected against radiation exposure from the buried waste.

References

Bollhöfer A & Doering C 2016. Long-term temporal variability of the radon-222 exhalation flux from a landform covered by low uranium grade waste rock. *Journal of Environmental Radioactivity* 151, 593–600.

Bollhöfer A, Doering C & Fox G 2015. Gamma dose rates and ^{222}Rn activity flux densities at the El Sherana containment. Internal Report 642, Supervising Scientist, Darwin.

Bollhöfer A, Doering C, Medley P & da Costa L 2013. Assessment of expected maximum doses from the El Sherana airstrip containment, South Alligator River valley, Australia. Internal report 618, Supervising Scientist, Darwin.

Doering C, Bollhöfer A, Ryan B, Sellwood J, Fox T & Pfitzner J 2011. Baseline and post-construction radiological conditions at El Sherana airstrip containment, South Alligator River valley, Australia. Internal Report 592, Supervising Scientist, Darwin.

Doering C, Medley P & Chen J 2017. Gamma dose rates and radon-222 exhalation flux densities at El Sherana containment in 2017. Internal Report 635, August, Supervising Scientist, Darwin.

IAEA 2013. Measurement and calculation of radon releases from NORM residues. Technical Report Series No. 474, International Atomic Energy Agency, Vienna.

ICRP, 2007. The 2007 recommendations of the International Commission on Radiological Protection. ICRP Publication 103, Annals of the ICRP 37(2–4).

ICRU 1994. Gamma-ray spectrometry in the environment. ICRU Report 53, International Commission on Radiation Units and Measurements.

NHMRC 1993. *Code of practice for the near-surface disposal of radioactive waste in Australia (1992)*. Radiation Health Series No. 35, Australian Government Publishing Service, Canberra.

Porstendörfer J 1994. Properties and behaviour of radon and thoron and their decay products in the air. *Journal of Aerosol Science* 25(2), 219–263.

Spehr W & Johnston A 1983. The measurement of radon emanation rates using activated charcoal. *Radiation Protection in Australia* 1(3), 113–116.

Waggitt PW 2004. Uranium mine rehabilitation: the story of the South Alligator Valley intervention. *Journal of Environmental Radioactivity* 76, 51–66.

Appendix 1 Gamma and radon-222 measurements

Table A1 Gamma counts and dose rates and radon-222 exhalation flux densities measured on and around the El Sherana containment in May/June 2019

Easting	Northing	Gamma counts (cpm)	Gamma dose rate (µGy h^{-1})	^{222}Rn flux density (mBq m^{-2} s^{-1})
On containment				
228872	8506246	112	0.10 ± 0.01	1.11 ± 1.29
228832	8506235	145	0.13 ± 0.01	1.42 ± 1.32
228756	8506272	139	0.12 ± 0.01	3.63 ± 0.91
228834	8506211	139	0.12 ± 0.01	12.9 ± 2.1
228786	8506259	129	0.11 ± 0.01	6.84 ± 0.98
228785	8506251	125	0.11 ± 0.01	2.36 ± 0.89
228737	8506258	136	0.12 ± 0.01	5.30 ± 1.58
228817	8506216	157	0.14 ± 0.01	19.2 ± 1.2
228792	8506235	115	0.10 ± 0.01	3.35 ± 1.45
228740	8506267	147	0.13 ± 0.01	4.86 ± 1.56
228789	8506229	150	0.13 ± 0.01	0.85 ± 1.32
228749	8506277	124	0.11 ± 0.01	16.7 ± 1.2
228771	8506233	140	0.12 ± 0.01	7.20 ± 1.73
228826	8506224	118	0.10 ± 0.01	2.23 ± 0.87
228758	8506235	148	0.13 ± 0.01	3.82 ± 0.91
228795	8506245	120	0.11 ± 0.01	-
228739	8506250	163	0.14 ± 0.01	4.10 ± 1.50
228804	8506242	102	0.09 ± 0.01	1.58 ± 0.86
228740	8506259	125	0.11 ± 0.01	2.76 ± 1.41
228760	8506241	161	0.14 ± 0.01	7.53 ± 1.75
228745	8506247	142	0.13 ± 0.01	4.64 ± 0.93
228761	8506263	133	0.12 ± 0.01	8.48 ± 1.02
228838	8506227	136	0.12 ± 0.01	1.00 ± 1.33
228782	8506230	124	0.11 ± 0.01	2.49 ± 1.41
228755	8506243	129	0.11 ± 0.01	1.55 ± 1.32
228823	8506252	154	0.14 ± 0.01	49.1 ± 1.8
228751	8506247	150	0.13 ± 0.01	2.63 ± 0.88
228773	8506257	120	0.11 ± 0.01	1.28 ± 1.32
228844	8506205	154	0.14 ± 0.01	11.3 ± 1.1
228810	8506258	117	0.10 ± 0.01	0.48 ± 0.83
Off containment				
228864	8506165	137	0.12 ± 0.01	1.96 ± 0.87
228812	8506300	125	0.11 ± 0.01	2.62 ± 1.40
228712	8506241	134	0.12 ± 0.01	1.58 ± 1.34

228815	8506176	140	0.12 ± 0.01	0.95 ± 1.27
228758	8506231	144	0.13 ± 0.01	0.36 ± 1.23
228877	8506207	131	0.12 ± 0.01	2.31 ± 1.38
228755	8506214	133	0.12 ± 0.01	3.69 ± 0.91
228701	8506344	114	0.10 ± 0.01	0.96 ± 1.28
228685	8506275	129	0.11 ± 0.01	1.42 ± 0.85
228754	8506205	153	0.14 ± 0.01	0.06 ± 1.22
228867	8506278	124	0.11 ± 0.01	1.62 ± 0.85
Outside fence				
228640	8506210	132	0.12 ± 0.01	0.37 ± 0.83
228889	8506120	189	0.17 ± 0.01	0.53 ± 1.28
228676	8506199	137	0.12 ± 0.01	1.92 ± 1.39
228742	8506174	102	0.09 ± 0.01	0.96 ± 1.28
228814	8506143	145	0.13 ± 0.01	4.69 ± 0.93